ELSEVIER

Ceramics International 30 (2004) 555–565

CERAMICS INTERNATIONAL

www.elsevier.com/locate/ceramint

New phase formation in Al_2O_3-based thermal spray coatings

M. Uma Devi*

Laboratory for Surface Engineering, University of Siegen, D-57068, Siegen, Germany

Received 3 April 2003; received in revised form 24 April 2003; accepted 15 July 2003

Abstract

Alumina phases formed in Al_2O_3 coatings and nanocomposite coatings of Al_2O_3–SiC, Al_2O_3–Mo were investigated. The coatings were prepared using high velocity oxy fuel spraying (HVOF) and air plasma spraying (APS) techniques on mild steel substrate either with Ni5Al or Ni20Cr bond layer. The amount of SiC and Mo were varied from 2 to 8 and 12 to 22 mass%, respectively. X-ray diffraction technique was used for phase characterisation. All the coatings showed the presence of varied amounts of well-known alumina phases, α- and γ-Al_2O_3, in the as-sprayed condition and after heat treatment up to 700 °C. In addition, a new highly oriented phase, referred to as U phase and characterised by an orthorhombic unit cell with $a = 8.644$ Å, $b = 8.286$ Å, $c = 4.922$ Å, was observed in all the alumina-based coatings. In as-sprayed condition, the U phase appeared in all the coatings prepared with Ni5Al bond layer and not in others. The new phase developed in other coatings, without bond layer or with Ni20Cr bond layer, under favourable energetics, i.e., after mild heat treatment at temperature as low as 100 °C and even due to mechanical stresses induced during cutting or peeling.

Keywords: B. Nanocomposites; B. X-ray methods; Thermal spray coatings

1. Introduction

Alumina has a number of metastable phases in addition to the thermally stable rhombohedral α-alumina or corundum phase. The metastable alumina polymorphs include γ (cubic spinel), δ (either tetragonal or orthorhombic), θ (monoclinic), η (cubic spinel), κ (orthorhombic), χ (cubic), β (hexagonal) and θ (monoclinic) [1–3]. These polymorphs can be obtained by dehydration of different alumina hydroxides, rapid quenching from the melt, vapour deposition, thermal spraying and crystallisation of amorphous alumina. All metastable aluminas (also termed as transition aluminas) have reproducible crystal structures and are stable at room temperature. The crystalline forms of alumina are constructed of stacked, close packed layers of oxygen ions with aluminium ions and the vacancies distributed on the tetrahedral and octahedral sites within the oxygen ions. The polymorphism results from the possibilities for different oxygen layer stacking sequences and from the variations in the distribution of aluminium ions on tetrahedral and octahedral sites and from the ordering of aluminium ions and vacancies on these sites.

There is considerable interest in understanding formation of alumina phases in the coatings prepared by thermal spraying (e.g., flame spraying [4–8] plasma [4–6,9–18]) and other techniques [19–21] to tailor their processing and properties. Large number of variables in terms of coating techniques, operating parameters, feed characteristics, substrate and post-coating treatment make the entire gamut of alumina phase formation very complex. Flame sprayed alumina coatings were reported to contain predominantly metastable γ-Al_2O_3 in addition to the equilibrium α-Al_2O_3 phase [4–6]. Plasma as-sprayed alumina coatings from commercial α-Al_2O_3 feedstock additionally showed presence of δ-Al_2O_3 [6,10]. Sokolova et al. [12] used α-Al_2O_3 powder of 25–50 μm size (60%) as feedstock and reported, that depending upon plasma spraying conditions either γ-Al_2O_3 or δ- and α-Al_2O_3 are formed in the coating. Measurement of particle temperatures in spray systems has shown that with an increase in particle size the fraction of partially melted particles increases rapidly with associated increase in α-Al_2O_3 phase [15]. Formation of α-Al_2O_3 from unmelted seeds and γ-Al_2O_3 from molten alumina is indicated during plasma spraying [6,9,12,13,15]. Attempts have also been

* Tel.: +49-271-740-4646; fax: +49-271-740-2442.
E-mail address: mu_devi@rediffmail.com (M. Uma Devi).

0272-8842/$30.00
doi:10.1016/j.ceramint.2003.07.002

Table 1
Spraying parameters used during HVOF and APS processes

	HVOF	APS
Gun	Top gun	Sulzer Metco 9 MB (30 kW power level)
Fuel/plasma gas	Ethylene	Ar + H_2
Spray distance (mm)	180 mm (Al_2O_3–SiC)	70 mm (Al_2O_3, Al_2O_3–SiC)
	200 mm (Al_2O_3, Al_2O_3–Mo)	100 mm (Al_2O_3–Mo)

made to alter the phase constitution of plasma-based alumina coatings through addition of another oxide [6,9,11] or non-oxide constituent, such as SiC [10].

In this paper results are presented on a previously unknown, highly oriented alumina phase (henceforth referred to as U phase), formed in Al_2O_3 and Al_2O_3–SiC, Al_2O_3–Mo nanocomposite coatings that are prepared on mild steel substrates using high velocity oxy fuel spray (HVOF) and air plasma spray (APS) techniques. The effect of different bond coats, Ni5Al and Ni20Cr, is investigated.

2. Experimental

The Al_2O_3–SiC feed stock powders, containing 2, 4 and 8 mass% (i.e., 2.5, 5 and 10 vol.%) of α-SiC, were produced by high-energy attrition milling (mechanical alloying) and agglomeration. Preparation of Al_2O_3–Mo feed stock (12 and 22 mass% Mo) was also carried out by mechanical alloying and subsequent agglomeration. Agglomeration was carried out by spray drying process, which transformed the angular as-milled powders into spherical agglomerates. Typical particle size distribution of Al_2O_3–4SiC feedstock had following size characteristic: $d_{0.1} = 2.2\,\mu m$, $d_{0.5} = 9.1\,\mu m$, $d_{0.9} = 19.3\,\mu m$. Whereas Al_2O_3–12Mo feed stock was a $-32\,\mu m$ fraction from a particle size distribution of $d_{0.1} = 14\,\mu m$, $d_{0.5} = 27\,\mu m$, $d_{0.9} = 57\,\mu m$.

The coatings of Al_2O_3–SiC and Al_2O_3–Mo were prepared on mild steel (S355JO) substrates using HVOF and air plasma spray (APS) techniques. Flat (3.7 cm × 7.5 cm) and roller (4 cm diameter) geometries were used for the substrates. Before spraying the substrates were blasted with 600–800 # (DIN) alumina grit at 5 bar pressure to get a surface roughness of 32–50 μm (R_z) and cleaned. In the preparation of all the investigated coatings, feed stocks were injected internally, with no tilt relative to the torch axis. During spraying the coating temperature was limited by blowing compressed air. The spray parameters are given in Table 1. Ni5Al or Ni20Cr was used for the bond layer. Pure alumina coatings prepared by HVOF (feed stock: $d_{0.5} = 5\,\mu m$, $d_{0.9} = 22\,\mu m$) and APS (classified, $-32\,\mu m$ powder) were used as reference. Five series of coatings of each composition were prepared with different thickness of top layer and 50 μm thick bond coats. The characteristics of the coated specimens used are summarised in Table 2. The specimens are designated as A-*n*, S_m-*n* and M_m-*n*. 'A', 'S' and 'M' represents Al_2O_3, Al_2O_3–SiC and Al_2O_3–Mo coatings, respectively. The subscript *m* signifies the mass% of second phase in Al_2O_3–SiC and Al_2O_3–Mo coatings. '*n*' indicate type of coating technique ($n = 1$–3: HVOF coating, $n = 4$–5: APS coatings) and bond coat ($n = 2$, 3, 5: Ni20Cr, and $n = 1$, 4: Ni5Al bond coat): A-0 is APS alumina coatings without any bond coat.

Seifert PTS X-ray diffractometer (XRD) is used for diffraction measurements using Cu Kα radiation at 50 kV and 39 mA with Ni filter and without monochromator. XRD

Table 2
Characteristics of the specimens (all top/bond coating compositions are expressed in mass%)

Sample code	Sprayed material	Spray process	Top coat thickness	Bond coat (thickness = 50 μm)
A-1	α-Alumina	HVOF	250 μm	Ni5Al
A-2	α-Alumina	HVOF	250 μm	Ni20Cr
A-4	α-Alumina	APS	250 μm	Ni5Al
A-0	α-Alumina	APS	250 μm	No
S_2-1	Agglomerate of (α-Al_2O_3 + 2 mass% SiC)	HVOF	250 μm	Ni5Al
S_2-2	Agglomerate of (α-Al_2O_3 + 2 mass% SiC)	HVOF	250 μm	Ni20Cr
S_2-3	Agglomerate of (α-Al_2O_3 + 2 mass% SiC)	HVOF	1 mm	Ni20Cr
S_2-4	Agglomerate of (α-Al_2O_3 + 2 mass% SiC)	APS	250 μm	Ni5Al
S_4-1	Agglomerate of (α-Al_2O_3 + 4 mass% SiC)	HVOF	250 μm	Ni5Al
S_4-2	Agglomerate of (α-Al_2O_3 + 4 mass% SiC)	HVOF	250 μm	Ni20Cr
S_4-3	Agglomerate of (α-Al_2O_3 + 4 mass% SiC)	HVOF	1 mm	Ni20Cr
S_4-4	Agglomerate of (α-Al_2O_3 + 4 mass% SiC)	APS	250 μm	Ni5Al
S_8-1	Agglomerate of (α-Al_2O_3 + 8 mass% SiC)	HVOF	250 μm	Ni5Al
S_8-2	Agglomerate of (α-Al_2O_3 + 8 mass% SiC)	HVOF	250 μm	Ni20Cr
S_8-3	Agglomerate of (α-Al_2O_3 + 8 mass% SiC)	HVOF	1 mm	Ni20Cr
S_8-4	Agglomerate of (α-Al_2O_3 + 8 mass% SiC)	APS	250 μm	Ni5Al
M_{12}-2	Agglomerate of (α-Al_2O_3 + 12 mass% Mo)	HVOF	250 μm	Ni20Cr
M_{12}-5	Agglomerate of (α-Al_2O_3 + 12 mass% Mo)	APS	250 μm	Ni20Cr
M_{22}-2	Agglomerate of (α-Al_2O_3 + 22 mass% Mo)	HVOF	250 μm	Ni20Cr
M_{22}-5	Agglomerate of (α-Al_2O_3 + 22 mass% Mo)	APS	250 μm	Ni20Cr

Table 3
Phase analysis of Al_2O_3 and Al_2O_3–SiC, Al_2O_3–Mo as-sprayed coatings prepared by HVOF and APS processes

Coating	Spraying technique	Bond layer	
		Ni20Cr	Ni5Al
Al_2O_3	APS	$\gamma + \alpha + \delta$[a]	$\gamma + \alpha + U + \delta$
Al_2O_3	HVOF	$\gamma + \alpha$	$\gamma + \alpha + U$
Al_2O_3–2% SiC	APS	–	$\gamma + \alpha + U$
Al_2O_3–2% SiC	HVOF	$\alpha + \gamma$	$\alpha + \gamma + U$
Al_2O_3–4% SiC	APS	–	$\gamma + \alpha + U + SiC$
Al_2O_3–4% SiC	HVOF	$\alpha + \gamma + SiC$	$\alpha + \gamma + U + SiC$
Al_2O_3–8% SiC	APS	–	$\gamma + \alpha + U + SiC$
Al_2O_3–8% SiC	HVOF	$\alpha + \gamma + SiC$	$\alpha + \gamma + U + SiC$
Al_2O_3–12% Mo	APS	$\alpha + Mo + \gamma$	–
Al_2O_3–12% Mo	HVOF	$\alpha + Mo + \gamma$	–
Al_2O_3–22% Mo	APS	$\alpha + Mo + \gamma$	–
Al_2O_3–22% Mo	HVOF	$\alpha + Mo + \gamma$	–

[a] Result for Al_2O_3 coating without any bond coating (sample A-0).

measurements were carried out, on the coatings along with the substrate, peeled free-forms, and free-forms powdered to −90 μm size. Coatings with substrate were examined without any heat treatment and after heat treatment at 100 and 700 °C for different length of time, ranging from 0.5 to 5.5 hour (h), and air-cooled. Phase indexing of unknown phase was carried out by "analyze" index/refine software of Agfa NDT Pantak Seifert GmbH & Co. KG. By applying dichotomy procedure [15] a search strategy for solutions from high to low symmetries (except the triclinic) is used while scanning through successive 400 Å shells of volumes.

3. Results and discussion

3.1. The new phase

The results of X-ray studies on thermally sprayed Al_2O_3, Al_2O_3–SiC and Al_2O_3–Mo coatings are summarised in Tables 3 and 4 under different conditions. Presence of a new highly oriented phase, designated as U phase, was found in the HVOF and APS coatings. As discussed in the subsequent sections, the occurrence/appearance of the U phase was found to be dependent on factors such as, bond coat, mechanical stress to cut/peel off the coating, thermal treatment, etc.

Table 5
Indexing of U phase (Cu Kα radiation λ = 1.5418, Ni filter)

No.	$h\,k\,l$	$2\theta_{obs}$	d_{obs}	d_{cal}	Relative intensity
1	0 2 0	21.450	4.139	4.143	v. Weak
2	2 1 0	23.157	3.838	3.832	Weak
3	2 1 1	29.507	3.025	3.024	v.v. Strong
4	3 0 1	36.099	2.486	2.487	Medium
5	1 1 2	39.498	2.279	2.276	Medium
6	4 1 0	43.283	2.089	2.091	Medium
7	4 1 1	47.199	1.924	1.925	Weak
8	4 2 0	47.344	1.919	1.916	Weak
9	0 4 1	47.595	1.909	1.909	Medium
10	3 0 2	48.634	1.871	1.871	Medium
11	2 2 3	64.793	1.438	1.438	v. Weak

Crystal system—orthorhombic, $a = 8.644$ Å, $b = 8.286$ Å, $c = 4.922$ Å, cell volume = 352.52 Å^3. Figures of merit: $M = 8.86$, $F = 3.88$.

The U phase diffraction peaks are given in Table 5. The U phase has a characteristic XRD pattern that is distinct from any of the transition aluminas reported in recent literature [2,3,22,23]. Indexing was carried out according to Louer & Louer [24] on the XRD data of alumina peeled free-form, heat treated at 1500 °C for 1 h. For U phase indexing the coating (with high temperature heat treatment) was so chosen that all metastable alumina polymorphs do not exist. The results are also presented in Table 5 in terms of observed and calculated d-spacing and the [$h\,k\,l$] indices assigned to different X-ray reflections. The crystal system is found to be orthorhombic with lattice parameters $a = 8.644 \pm 0.00488$ Å, $b = 8.286 \pm 0.00750$ Å, $c = 4.922 \pm 0.00311$ Å, and cell volume = 352.52 Å^3.

3.1.1. Occurrence in as-sprayed coatings

Typical XRD patterns for the as-sprayed Al_2O_3 and Al_2O_3–SiC coatings prepared by different spray techniques are given in Figs. 1 and 2, respectively. Whereas X-ray

Table 4
Typical phase analysis results on Al_2O_3 coating and Al_2O_3–SiC, Al_2O_3–Mo nanocomposite coatings showing effect of heat treatment at 100 °C for different time

Coating	Spraying technique	Alumina phases formed after different time						
		0[a]	30 min	1 h	2 h	2.5 h	5 h	5.5 h
(a) Coatings with Ni20Cr bond layer containing no U phase [coating thickness: 250 μm]								
Al_2O_3	HVOF	$\gamma + \alpha$	$\alpha + \gamma + U$[b]	$\alpha + \gamma + \delta$	$\alpha + \gamma + \delta$	$\alpha + \gamma + U$	–	$\alpha + \gamma + U$
Al_2O_3–4% SiC	HVOF	$\alpha + \gamma$	$\alpha + \gamma + U$	$\alpha + \gamma + U$	$\alpha + \gamma + U$	$\alpha + \gamma + U$	–	$\alpha + \gamma + U$
Al_2O_3–12% Mo	HVOF	$\alpha + \gamma$	–	–	–	$\alpha + \gamma + U$	$\alpha + \gamma + U$	$\alpha + \gamma + U$
(b) Coatings with Ni5Al bond layer containing U phase [coating thickness: 250 μm]								
Al_2O_3–4% SiC	APS	$\gamma + \alpha + U$	$\gamma + \alpha + U$	$\gamma + \alpha + U$	–	–	$\gamma + \alpha + U$[c]	–
Al_2O_3–4% SiC	HVOF	$\alpha + \gamma + U$	$\alpha + \gamma$	$\alpha + \gamma$	$\alpha + \gamma$	–	$\alpha + \gamma + U$	–

[a] Phases in as-sprayed coating.
[b] Un-textured U phase.
[c] Heat treatment time 4 h.

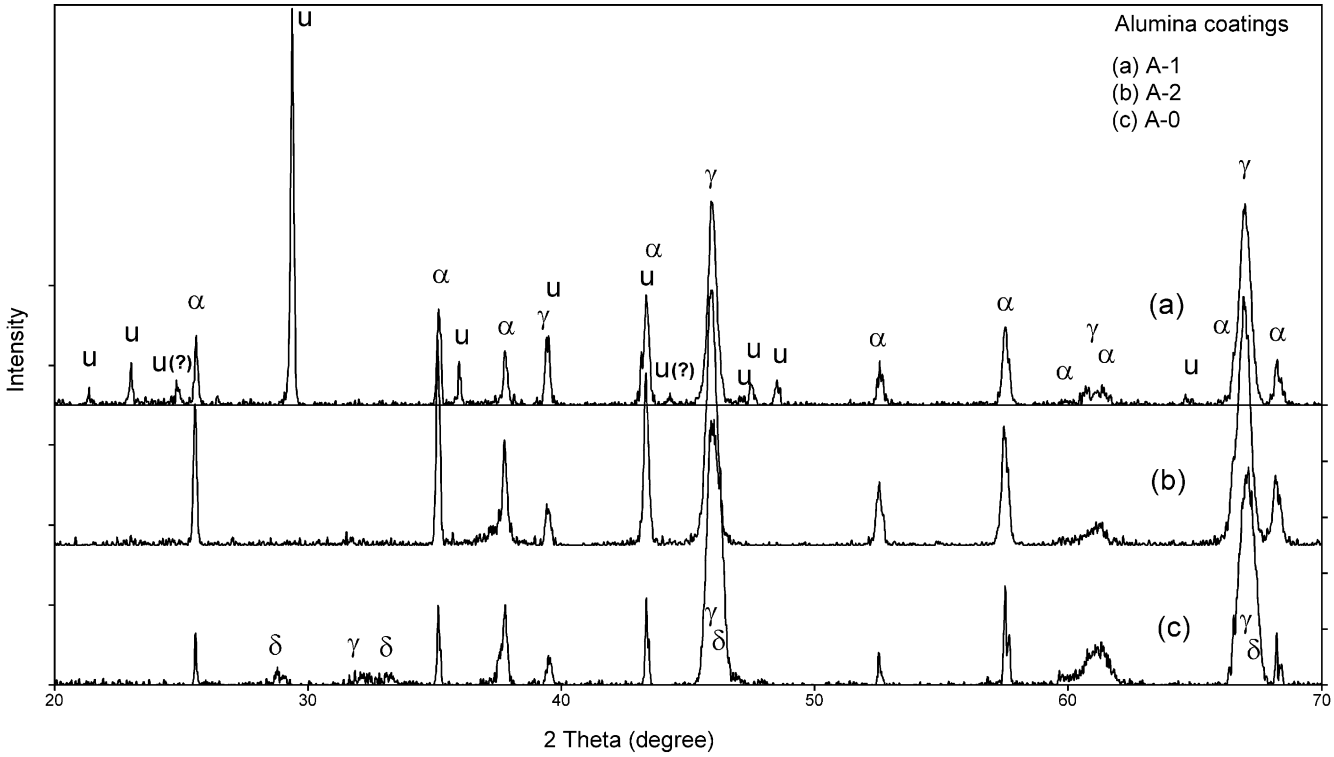

Fig. 1. XRD patterns of alumina coatings prepared with different thermal spray techniques (APS & HVOF) and bond-coats.

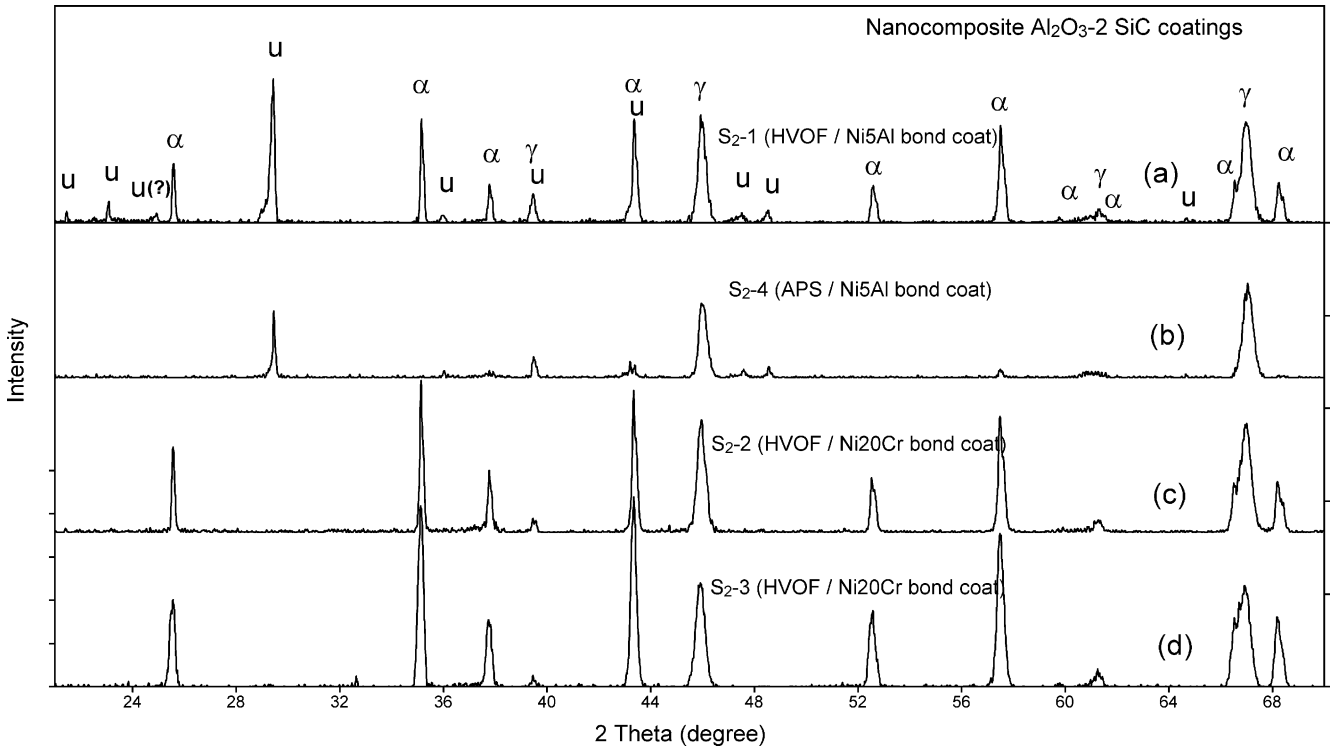

Fig. 2. XRD patterns of nanocomposite ceramic coating (S_2 series) prepared with different thermal spray techniques (APS & HVOF) and bond coats.

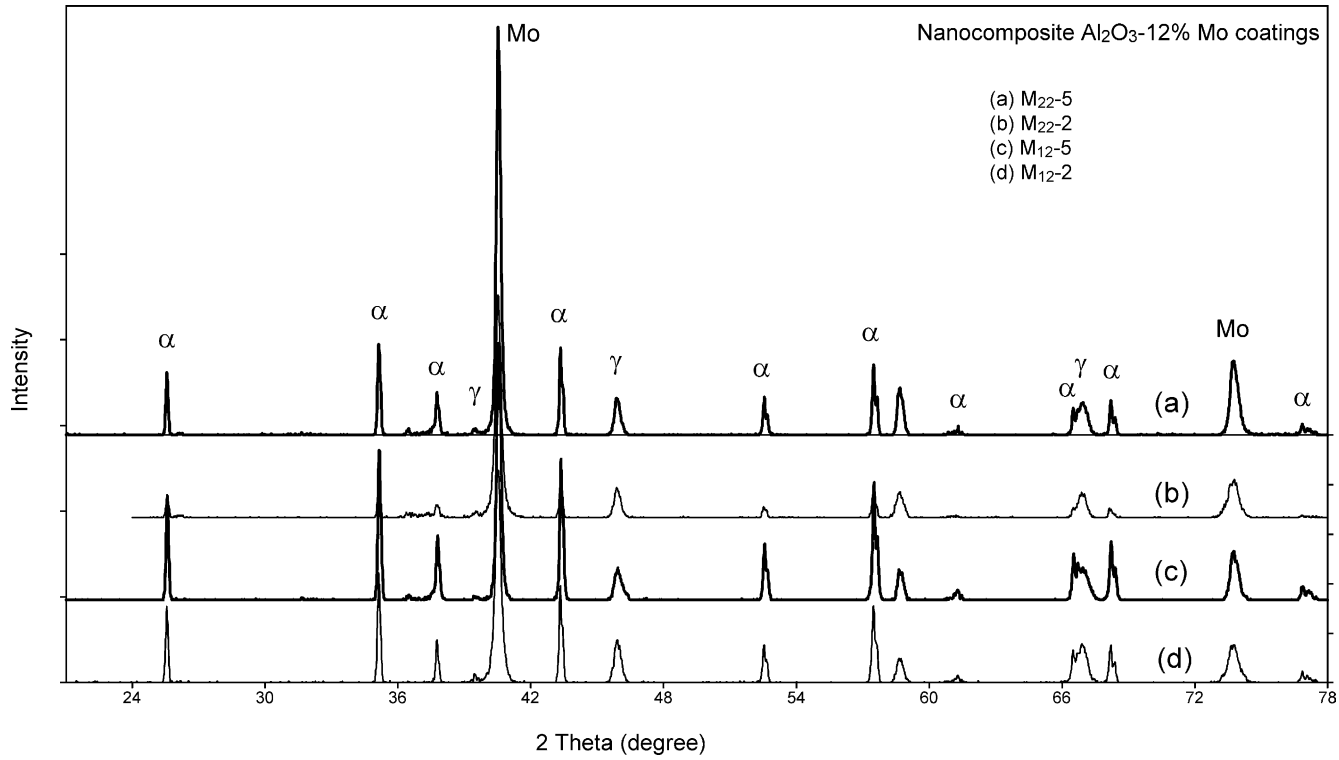

Fig. 3. XRD patterns of nanocomposite coating (M series) prepared with different thermal spray techniques (APS & HVOF).

diffractograms of Al_2O_3–Mo coatings prepared by HVOF and APS techniques are shown in Fig. 3. The results of the phase analysis are summarised in Table 3 to elucidate the effect of bond layer composition. Depending upon the bond layer composition, presence of the new phase U was detected in the Al_2O_3 as well as in the nanocomposite Al_2O_3–SiC coatings prepared by HVOF and APS (Figs. 1 and 2, Table 3). The alumina coatings made by APS without bond layer (Fig. 1(c)), and the ones made by HVOF spray process with Ni20Cr as bond layer (Fig. 1(b)) showed the presence of $\gamma + \alpha + \delta$ and $\gamma + \alpha$ phases, respectively, in the as-sprayed condition. In sharp contrast, the alumina coating prepared with Ni5Al as bond layer has shown the presence of the new phase U, along with $\alpha + \gamma$ phases (Fig. 1(a)). Nanocomposite Al_2O_3–SiC (2–8 mass%) and Al_2O_3–Mo (12–22 mass%) coatings had shown similar behaviour (Table 3). The appearance of U phase in association with $\alpha + \gamma$ phases is observed in the coatings with Ni5Al bond layer, using either of the spray techniques (Fig. 2(a) and (b), Table 3). Absence of the U phase in the nanocomposite coatings prepared with Ni20Cr bond layer is evident from XRD patterns in Figs. 2(c), (d) and 3 and the results are presented in Table 3. In addition to the indexed X-ray reflections of U phase, 2/3 very weak reflections were also observed in the as-sprayed condition with Ni5Al bond-coat/prolonged low temperature heat treated coatings with Ni20Cr bond-coat (shown in the figures as U(?)). High quenching rates in HVOF and APS processes perhaps lead to some disorientation in the U phase. To find out reasons for the appearance of extra 2/3 weak reflections needs further investigation.

3.1.2. Characteristic features of the U phase

The U phase showed a number of characteristic features and these are described below:

(1) Effect of mechanical stress

The Al_2O_3 coatings (A-2), Al_2O_3–SiC and Al_2O_3–Mo nanocomposite coatings (S-2, S-3, M-2 and M-5) with Ni20Cr bond layer, which do not display U phase and showed only the presence of α- and γ-Al_2O_3 phases in the as-sprayed condition, were cut perpendicular to the coated surface to induce shear stresses into the residual coating stresses. XRD patterns at or near the cut surface were obtained for the samples. Typical XRD patterns in the as-sprayed and near the cut (for S_2-3) and peeled free-form (S_4-2) are given in Fig. 4. Appearance of U phase peaks at or near the cut surface and the absence in the as-sprayed condition is evident from the figure. It is interesting to note that the coatings which seem to contain no U phase in the as-sprayed condition developed U phase in the mechanically peeled free-form (XRD pattern of the peel of S_4-2 can be seen as part of Fig. 4).

(2) Effect of thermal treatment

Al_2O_3 coating and Al_2O_3–SiC, Al_2O_3–Mo nanocomposite coatings, which do not display U phase in the as-sprayed condition were heat treated at 700 °C

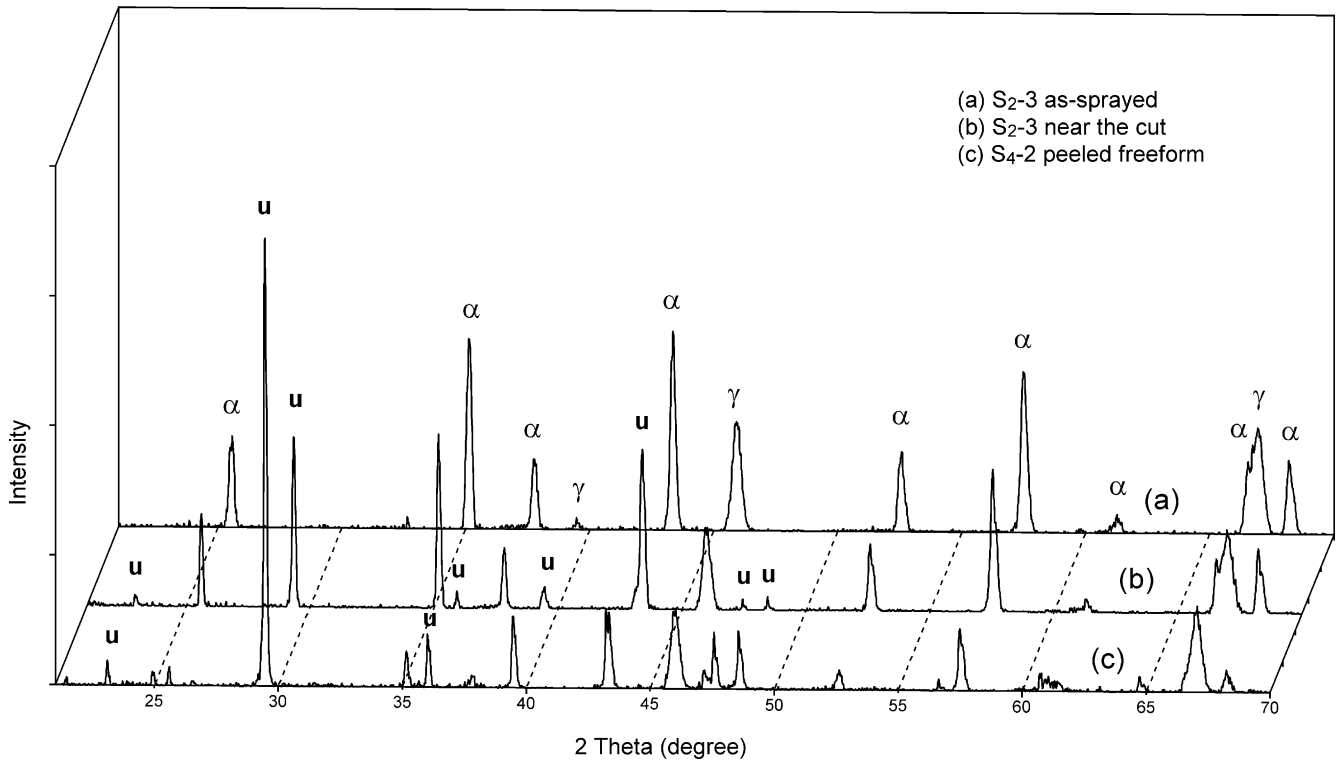

Fig. 4. XRD patterns of nanocomposite ceramic coatings (S_2-3) (HVOF/1 mm thick coating): (a) as-sprayed, (b) near the cut, (c) S_4-2 peeled free-form.

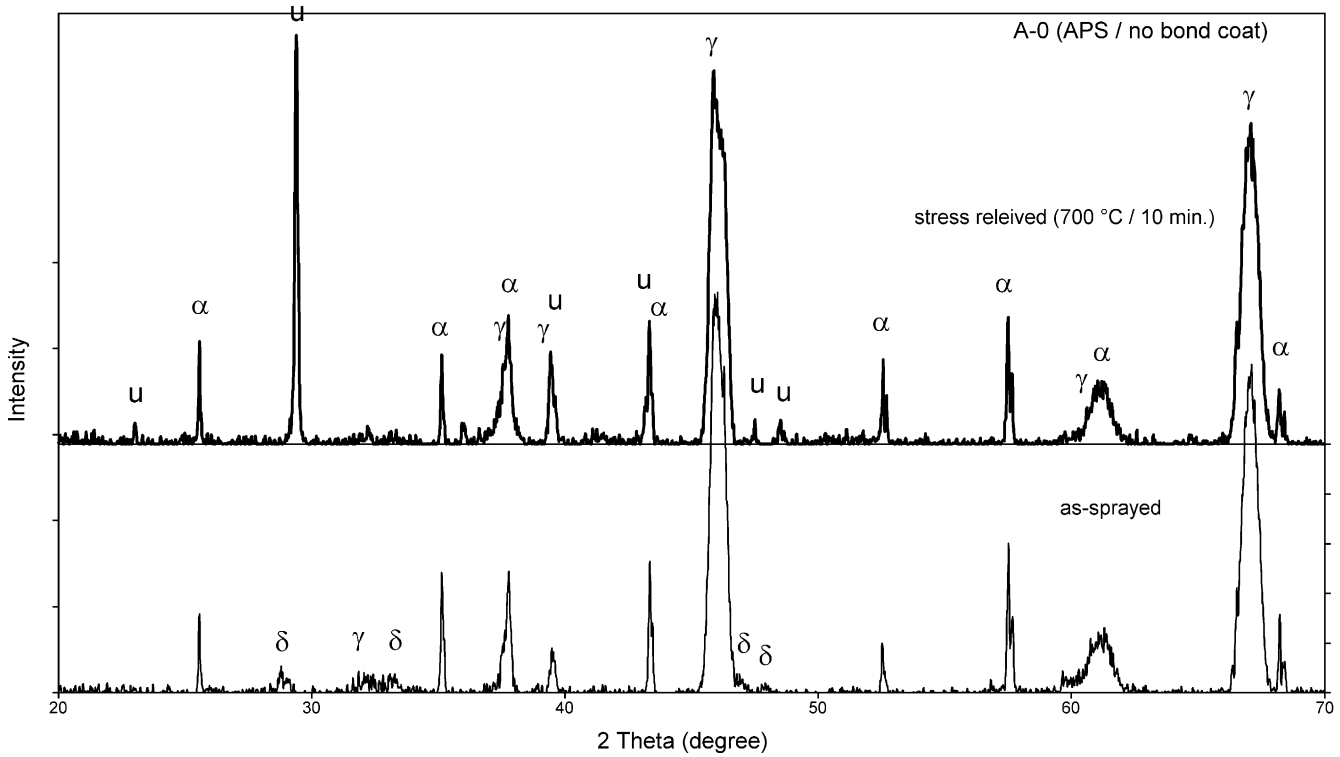

Fig. 5. XRD patterns of alumina coating (APS/no bond-coat), as-sprayed and stress relieved at 700 °C.

for 10 min. Typical XRD patterns for A-0 coating are given in Fig. 5, before and after the heat treatment. Presence of U phase after the thermal treatment and absence of it in the as-sprayed condition is evident from the presented results. Similar observations were made on alumina-based nanocomposite coatings.

From the above experimental results it follows that U phase appears to have no crystallinity (absence of long range order) under certain conditions, e.g., as-sprayed coatings prepared with Ni20Cr bond coat, and develops into a crystalline phase due to mechanical stress induced during cutting/peeling off of the coating or thermal treatment (stress relief) of the coatings.

It is not clear why U phase forms in as-sprayed condition with Ni5Al bond coat and not with Ni20Cr bond coat. Both the bond coats, Ni5Al and Ni20Cr are used to balance the difference between the coefficients of thermal expansion of the ceramic layer and the metal (steel) substrate. One possible explanation for the formation of U phase could be presence of aluminium bearing oxidised interface in Ni5Al bond coat and/or exothermic formation of intermetallic phases such as NiAl and $NiAl_3$. Recent studies by Yuanzheng et al. [17] on the interfaces in plasma sprayed (Al_2O_3–TiO_2 (13%)) coatings with NiCrAl bond layer have indicated possibility of the formation of Ni(Cr, Al)O at the interface (no detailed phase analysis results are reported). Presence of aluminium at the interface and the possibility of its self-bonding with the alumina that is deposited seems to result in *favourable energetics for the long range ordering of U phase* in as-sprayed coatings with Ni5Al bond coat. On the other hand self-bonding is not possible in the case of Ni20Cr bond layer, which has all dissimilar elements.

U phase is formed with Ni5Al bond layer in both HVOF as well as APS alumina-based coatings (Figs. 1 and 2). In order to further enhance our understanding about its formation, Al_2O_3 and alumina-based nanocomposite coatings with Ni20Cr bond layer were given thermal treatment at 100 °C for various lengths of time and examined by X-ray. The results of X-ray studies are summarised in Table 4. Typical X-ray diffraction patterns for the Al_2O_3, Al_2O_3–SiC and Al_2O_3–Mo HVOF coatings are shown in Figs. 6–8, respectively. The as-sprayed Al_2O_3 coating with Ni20Cr bond coat, which did not show the presence of U phase, developed U phase peaks even after short heat treatment of 30 min at 100 °C (Fig. 6). By extending the duration of the heat treatment, it recrystallised forming a highly textured U phase via δ phase (Table 4). Similar trend is observed with Al_2O_3–SiC and Al_2O_3–Mo nanocomposite coatings (Figs. 7 and 8, Table 4). With low temperature heat treatment, (100 °C/30 min), the U phase, which was not observed (no long range order) in the as-sprayed condition, favourably orient and give rise to diffraction peaks. With the application of prolonged heat treatment, the

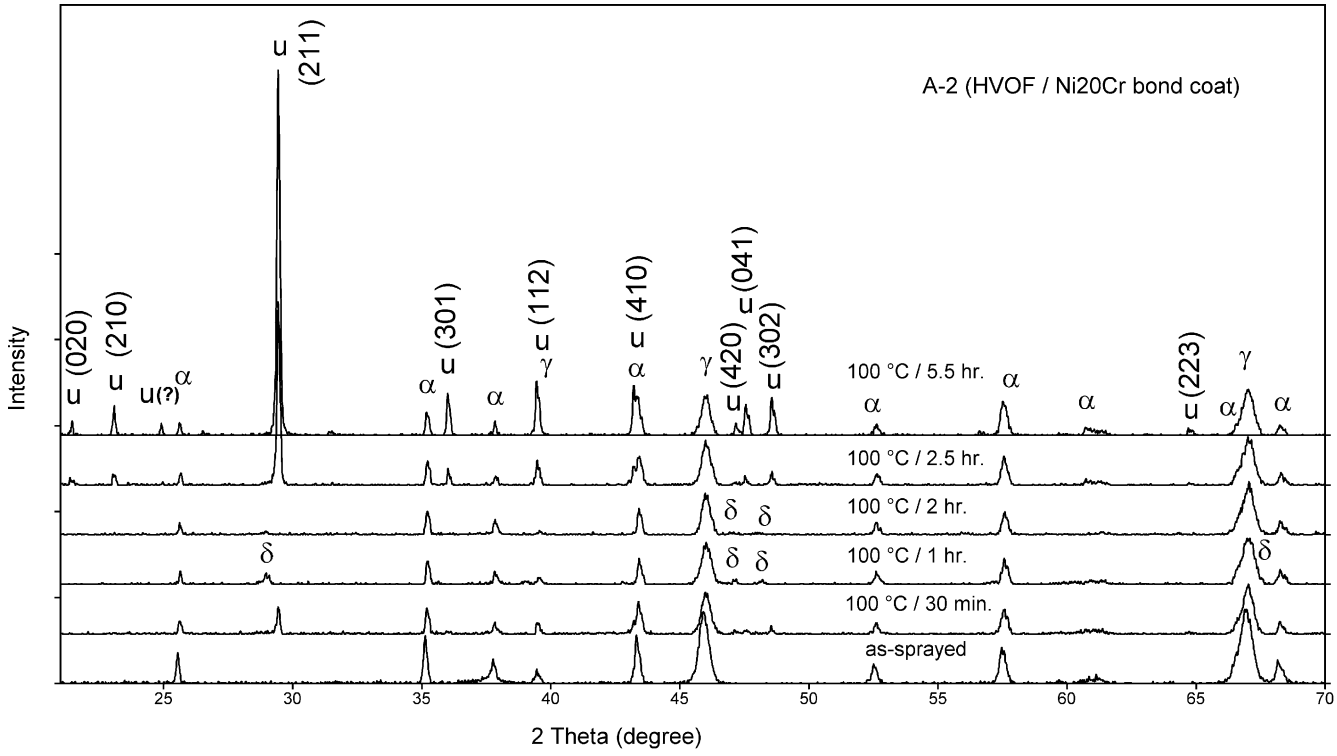

Fig. 6. XRD patterns of alumina coating (HVOF/Ni20Cr bond-coat) with low temperature (100 °C) heat treatments.

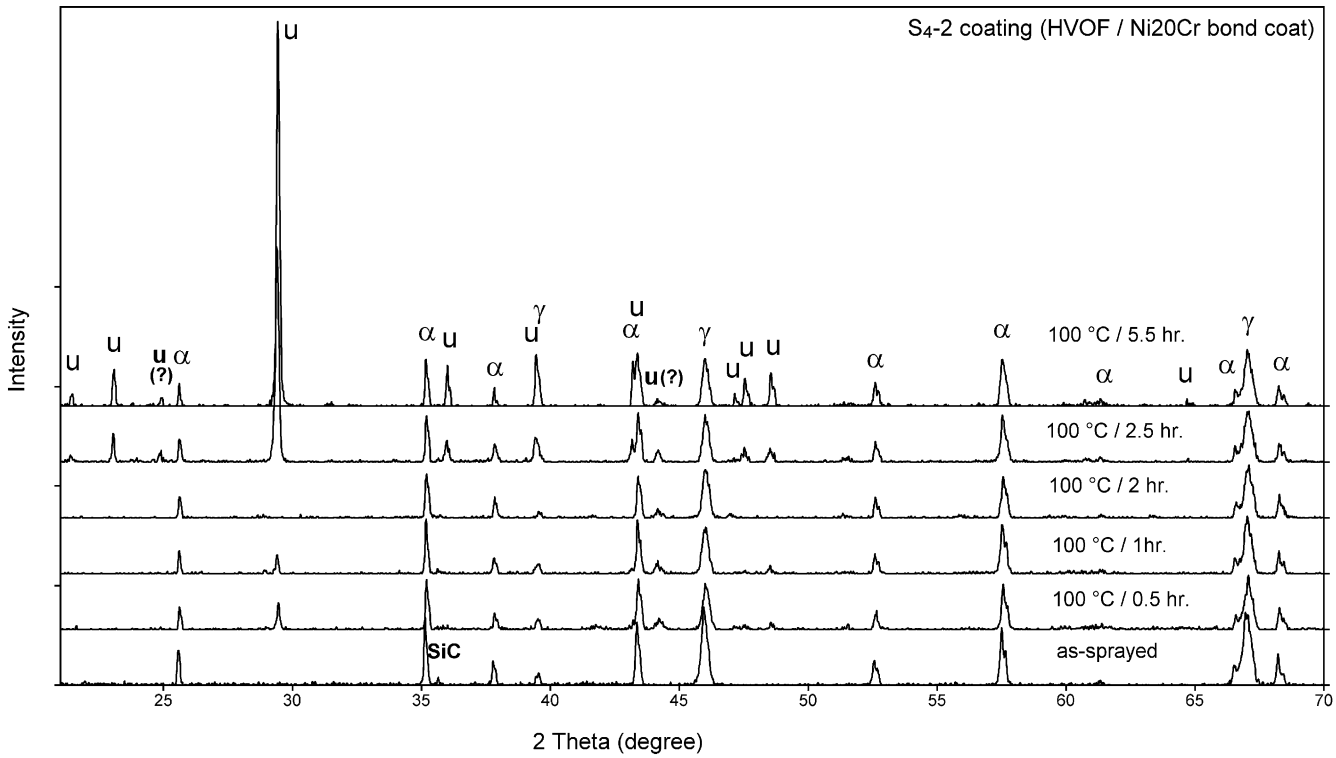

Fig. 7. XRD patterns of nanocomposite ceramic coating S_4-2 with low temperature (100 °C) heat treatments.

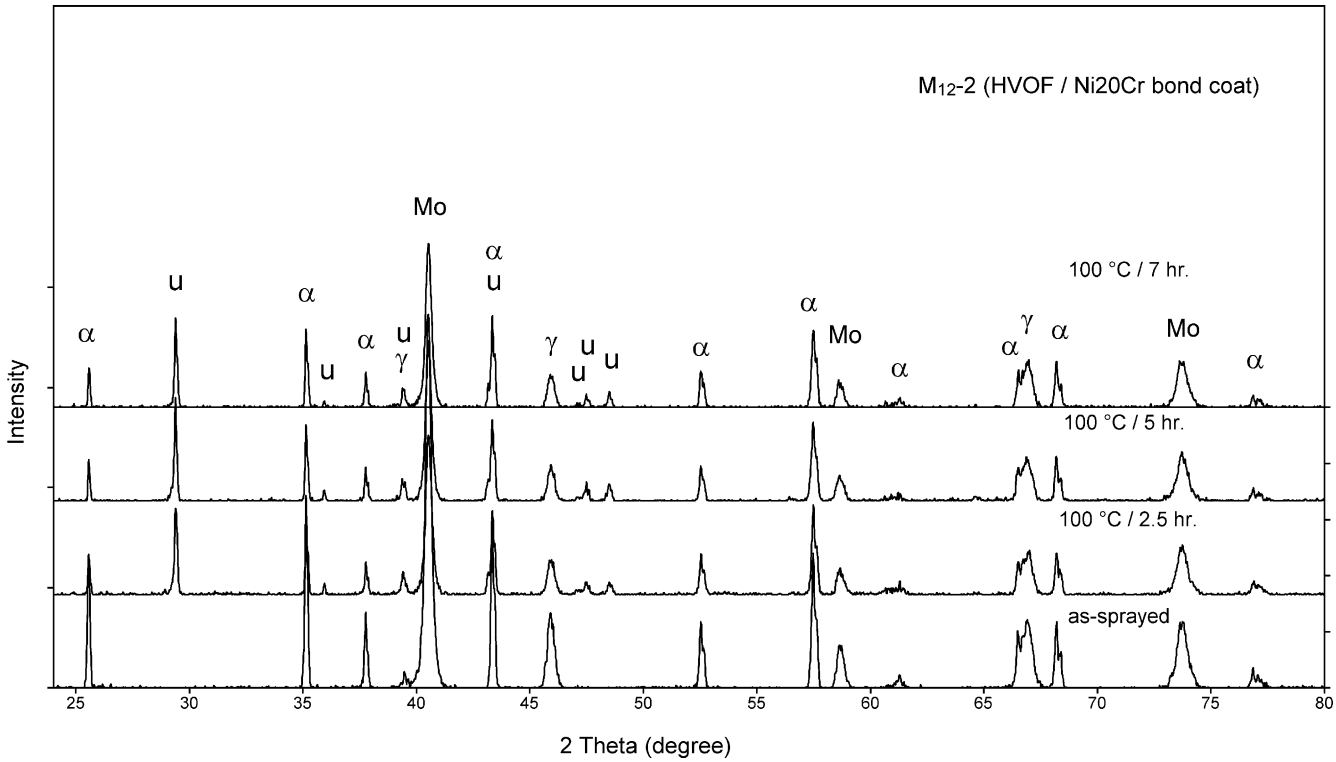

Fig. 8. XRD patterns of nanocomposite coating M_{12}-2 with low temperature (100 °C) heat treatments.

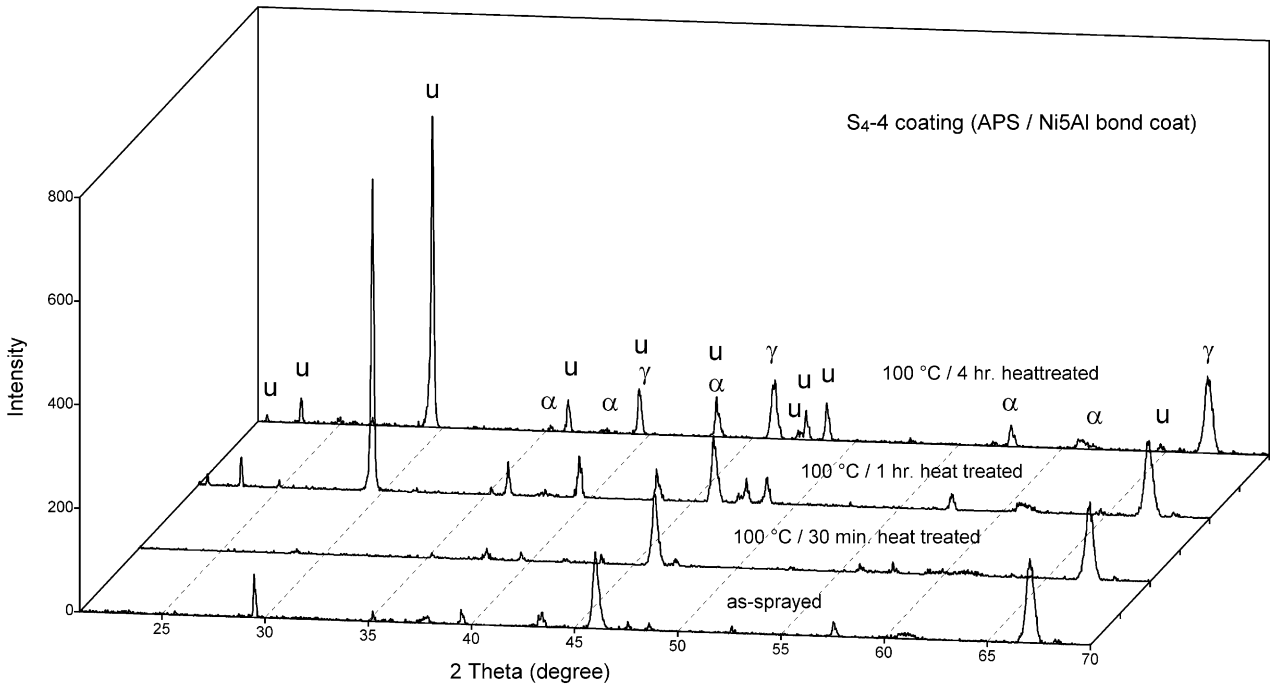

Fig. 9. XRD patterns of nanocomposite ceramic coating S_4-4 with low temperature (100 °C) heat treatments.

U phase further changes into a highly oriented phase (textured phase/(2 1 1) planes parallel to the splats).

Effect of heat treatment at 100 °C on the U phase was also investigated in Al_2O_3–SiC coatings with Ni5Al bond coat that were prepared by APS and HVOF (Table 4, Fig. 9). Typically, in APS coatings the U phase changed to a textured (2 1 1) phase after an hour heat treatment and the textured phase persisted

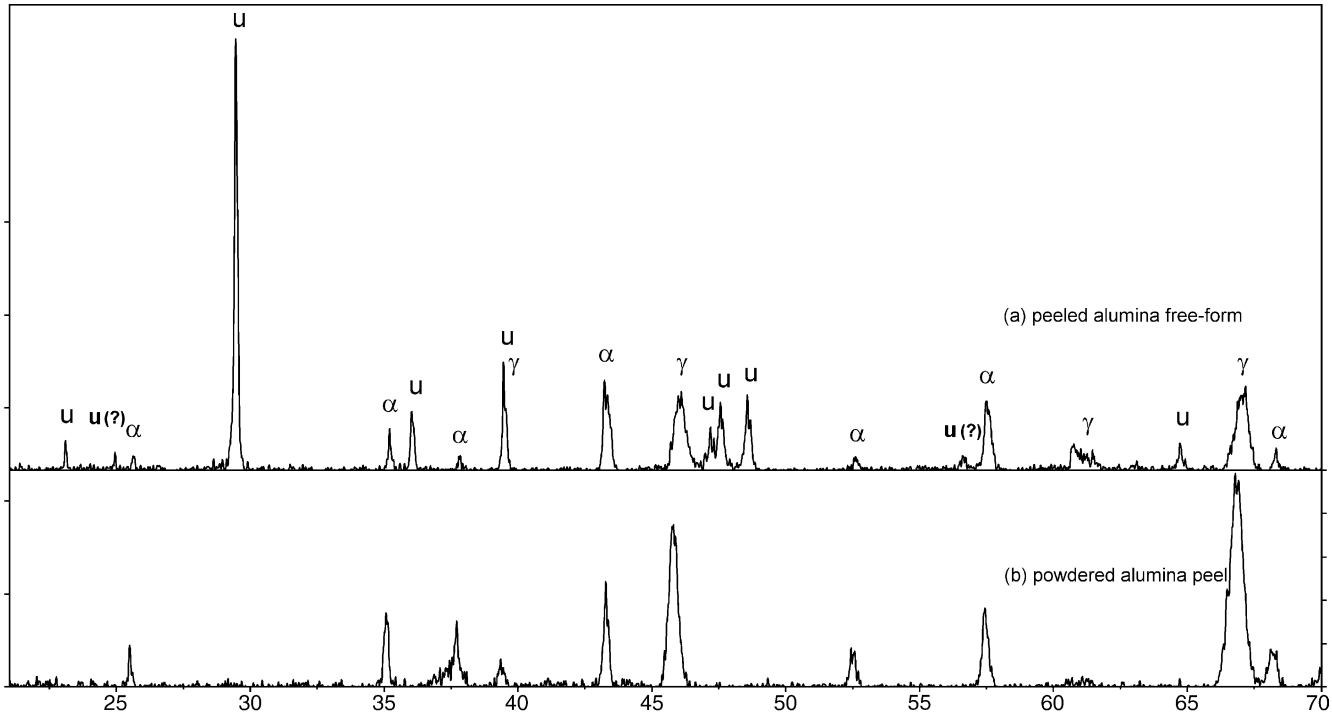

Fig. 10. XRD patterns of (a) peeled alumina (A-2) free-form and (b) its powder.

even with prolonged heat treatment (4 h). Similar results were obtained for HVOF coatings, however the textured U phase appeared in this case after prolonged heat treatment for 2.5 h.

(3) U phase forms at splat boundaries

U phase was thought to be forming at the splat boundaries. To verify this idea, the A-2 and S-2 peels were powdered and sieved to −90 μm size. Powdering was carried out to eliminate or destroy the splat boundaries. The powdered samples were examined by XRD. Typical results for A-2 peeled free-forms and its powder are shown in Fig. 10(a) and (b), respectively. The results obtained for S-2 and M-2 peels were similar to A-2 peels. Absence of U phase in the powdered alumina peel (Fig. 10(b)) seems to corroborate the hypothesis that U phase is a splat boundary phase. Heat treatment of powdered peels did not result in the development of U phase.

3.1.3. Omission of the U phase by other researchers

Most of the researchers [4–6,7,8,12,13,16] prepared thermal sprayed alumina coatings without any bond layer. Jiansirisomboon et al. [10] prepared Al_2O_3 and Al_2O_3–SiC nanocomposite coatings with Co32Ni21Cr8Al0.5Y_2O_3 bond layer using low pressure plasma spraying. Thompson and Whittemore [4] prepared APS alumina coatings on preheated stainless steel rod, coated with saturated solution of sodium chloride. Huffadine and Thomas [8] made dense α-alumina, flame sprayed on a removable semi-rigid carburised resin impregnated batt. Both the groups [4,8] have done heat treatments on the free forms at 1149 to above 1371 °C and 1250 to 1450 °C, respectively. Alumina coatings sprayed by Zoltowski [13] were also on removable core. The above three groups [4,8,13] worked with alumina forms made on removable core.

Our work indicates that the formation of U phase is dependent on a number of factors, e.g., sample preparation, bond coat, thermal treatment, etc. Previous researchers do not report the occurrence of U phase and this could be due to one or more of the following reasons:

(a) Use different bond coats, e.g., sodium chloride, resins, etc.
(b) State of the sample, for example the free-forms (A-2 and C-2) used in the present investigation were with Ni20Cr bond coat and peeled mechanically; these have a different stress state compared to the free-forms prepared with removable core.
(c) Sample preparation—U phase developed in coatings with Ni20Cr bond coat after heat treatment; removal of splat boundaries by powdering led to the disappearance of U phase.
(d) Different focus of the studies, for example Yuanzheng et al. [17] primarily examined bond-substrate and bond-coating interfaces by TEM in plasma sprayed Al_2O_3–TiO_2 coatings; Binanchi et al. [18] carried out atomic force microscopic investigations on plasma sprayed alumina splats; Mc Pherson and coworkers [14,15,25] primarily carried out theoretical analysis of the processes occurring during impact and solidification of sprayed alumina powders.

4. Conclusions

1. A new highly oriented phase, called U phase was detected in Al_2O_3 and nanocomposite Al_2O_3–SiC coatings prepared by HVOF and APS. U phase is indexed based on orthorhombic crystal system with lattice parameters $a = 8.644$ Å, $b = 8.286$ Å, $c = 4.922$ Å.
2. In as-sprayed condition, the U phase appeared in all the alumina-based coatings prepared with Ni5Al bond layer and not in others.
3. The new phase developed in other coatings, without bond layer or with Ni20Cr bond layer, after mild heat treatment at temperature as low as 100 °C and even due to mechanical stresses, induced during cutting.
4. U phase appears to be a splat boundary phase.

Acknowledgements

The work described in this paper was carried out whilst the author was on leave from Tata Steel, with the Laboratory for Surface Engineering, University of Siegen. Thanks are due to Tata Steel for providing the opportunity and the Laboratory for Surface Engineering (Prof. H. Weiss) for provision of facilities. Software (Analyxe/Index) service/facilities from Dr. Alfried Haase of Agfa NDT Pantak Seifert GmbH & Co. KG is gratefully acknowledged.

References

[1] K. Wefer, Misra, Alcoa Technical Paper No. 19, Alcoa Laboratories, 1987.
[2] I. Levin, L.A. Bendersky, D.G. Brandon, M. Rühle, Acta Mater. 45 (9) (1997) 3659–3669.
[3] P.S. Santos, H.S. Santos, S.P. Toledo, Mater. Res. 3 (4) (2000) 104–114.
[4] V.S. Thompson, O.J. Whittemore, Bull. Am. Ceram. Soc. 47 (1968) 637.
[5] V.F. Eichorn, J. Metzler, W. Eysel, Metalloberflache 26 (1972) 212 (in German).
[6] I.R. Kozlova, Izv. Akad. Nauk. S.S.S.R. Neorg. Mater. 7 (1971) 1372 (in Russian).
[7] D.G. Moore, A.G. Eubanks, H.R. Thornton, W.D. Hayes, A.W. Crigler, Technical Report No. A.R.L. 59, Contract AF 33 (616)-58-19 Final Summary Report, 1961.
[8] J.B. Huffadine, A.G. Thomas, Powder Metall. 7 (14) (1964) 290–299.
[9] L.L. Shaw, D. Goberman, R. Ren, M. Gell, S. Jiang, Y. Wang, T.D. Xiao, P.R. Strutt, Surf. Coat. Technol. 130 (2000) 1–8.
[10] S. Jiansirisomboon, K.J.D. MacKenzie, S.G. Roberts, P.S. Grant, J. Eur. Ceram. Soc. 23 (6) (2002) 961–976.

[11] R. Gansert, P. Chraska, J. Ilavsky, in: Proceedings of the MRS Fall Meeting on the Science and Technology of Thermal Spray Materials Processing, Boston, Paper No. BB5.2, 2–4 December 1997.
[12] T.V. Sokolova, I.R. Kozolva, Ch. Derko, A.V. Kijko, Izv. Akad. Nauk. S.S.S.R. Neorg. Mater. 9 (1973) 611 (in Russian).
[13] P. Zoltowski, Rev. Int. Hautes, Temp. Refract. 5 (1968) 253 (in French).
[14] R. Mc Pherson, J. Mater. Sci. 15 (1980) 3141–3149.
[15] A. Vardelle, M. Vardelle, R. Mc Pherson, P. Fauchais, in: Proceedings of the 9th International Thermal Spraying Conference, Netherlands Institute of Lastechnick, The Hague, Amsterdam, May 1980, p. 155.
[16] N.N. Ault, J. Am. Ceram. Soc. 40 (3) (1957) 69–74.
[17] Y. Yuanzheng, L. Zhiguo, L. Zhengyi, C. Yuzhi, Thin Solid Films 388 (2001) 208–212.
[18] L. Binanchi, A. Denoirjean, F. Blein, P. Fauchais, Thin Solid Films 299 (1997) 125–130.
[19] A.L. Dragoo, J.J. Diamond, J. Am. Ceram. Soc. 50 (1967) 568.
[20] R. Cremer, M. Witthaut, D. Neuschutz, G. Ekens, T. Leyendecker, M. Feldhege, Surf. Coat. Technol. 120/121 (1998) 213–218.
[21] O. Kyrlov, R. Cremer, D. Neuschutz, Surf. Coat. Technol. 163/164 (2003) 203–207.
[22] A.H. Carim, G.S. Rohrer, N.R. Dando, S.Y. Tzeng, C.L. Rohrer, A.J. Perrotta, J. Am. Ceram. Soc. 80 (10) (1997) 2677–2680.
[23] JCPDS X-ray Diffraction Files for Transition Alumina Phases, γ [29-1486, 29-0063, 10-0425], δ [16-0394, 04-0877], θ [35-0121, 11-0517, 23-1009], η [21-0010], κ [04-0878], χ [34-0493, 13-0373, 04-880].
[24] D. Louër, M. Louër, J. Appl. Cryst. 5 (1972) 271–275 (in French).
[25] R. Mc Pherson, J. Mater. Sci. 8 (1973) 851–858.